EMBJ.ORG FOR YOUNG DOCTORS

EUROMEDITERRANEAN BIOMEDICAL JOURNAL
2020,15 (46) 197–202
(*FORMERLY: CAPSULA EBURNEA*)

Original article

PERFORMANCE OF DIFFUSION KURTOSIS IMAGING FOR CHARACTERIZATION OF PROSTATE LESIONS USING 1.5T MAGNETIC RESONANCE IMAGING SCANNER

Gabriele Busè [1], Roberto Cannella [1], Alberto Bruno [1], Claudio Leto [1], Giuseppe Cutaia [1], Leonardo Salvaggio [1], Vincenzo Costanzo [1], Dario Giambelluca [1], Marcella Ferraro [1], Federica Vernuccio [1],Giorgio Collura [1,2], Cesare Gagliardo [1], Maurizio Marrale [1], Massimo Midiri [1], Massimo Galia [1], Giuseppe Salvaggio [1]

1. Sezione di Scienze Radiologiche, Dipartimento di Biomedicina, Neuroscienze e Diagnostica avanzata (BIND), University of Palermo, Via del Vespro 129, Palermo, Italy.
2. Dipartimento di Fisica e Chimica Emilio Segrè, University of Palermo, Italy.

ARTICLE INFO

Article history:
Received 25 September2020
Revised 03 November2020
Accepted 19 November 2020

Keywords:
Prostate Cancer, Gleason score, Magnetic Resonance Imaging, Apparent Diffusion Coefficient, Apparent Kurtosis Coefficient.

ABSTRACT

The aim of the study is to evaluate the diagnostic performance of apparent diffusion coefficient (ADC) and apparent kurtosis coefficient (Kapp) for the characterization of prostate lesions on 1.5T MRI. This retrospective study included 34 patients with at least one lesion with PI-RADS score≥ 3. Performances of ADC and Kapp were evaluated using the Mann-Whitney U test and receiver operating characteristics curve (AUROC). Lesions with Gleason score≥6 had significantly lower Kapp compared to benign lesions (p=0.025). The ADC-ratio was the only significantly different parameter between GS≥7 and GS=6 lesions (p=0.039). Kapp showed the largest AUROC for the diagnosis of GS≥6 prostate cancers (AUROC: 0.741, p=0.025), while the largest AUROC for the diagnosis of GS≥7 prostate cancers was achieved by the ADC-ratio (AUROC: 0.709, p=0.039). While Kapp demonstrated no significant benefit in characterization of prostate cancers compared to ADC, it could be helpful to distinguish benign lesions from prostate cancers.

1. Introduction

Magnetic resonance imaging (MRI) is considered the best imaging technique for the detection, staging and surveillance of prostate cancer due to its ability to provide functional and anatomic information [1]. Initially, prostate MRI was performed only with morphological/anatomical sequences (T1- and T2- weighted sequences) so that it could be used for locoregional staging in patients with biopsy-proved prostate carcinoma.

To date, prostate MRI is a multiparametric technique thanks to the introduction of functional sequences like diffusion weighted imaging (DWI) and its derivative apparent diffusion coefficient (ADC) maps, and dynamic contrast enhanced (DCE) sequences. Multiparametric MRI not only allows anatomical information [like zonal anatomy (Figure 1) but also provided capability to distinguish benign pathological tissue and clinically insignificant prostate cancer from significant cancer.

Among the functional techniques, diffusion weighted imaging (DWI) has a significant role since it allows evaluation of the capability of diffusion of water molecules in biological tissues, quantifiable through the calculation of the apparent diffusion coefficient (ADC).

However, the wide variability of measured ADC values in the prostate due to patient and technical factors has led investigators to use ADC-ratio, which is defined as ADC of the tumor divided by that of a reference area. Initial studies have shown controversial results with some of them reporting ADC-ratio superior to ADC in detection of prostate cancer and determination of tumor aggressiveness, while others have found no additional benefit from using ADC-ratio [2-6].

Furthermore, water in biological structures often exhibits a non-Gaussian diffusion behavior. Therefore, the DWI signal shows a more complex behavior that needs to be modeled following different approaches [7].

Diffusion kurtosis imaging (DKI) is a non-Gaussian diffusion weighted model first described by Jensen et al. [8] in 2005 that is believed to better reflect the microstructural complexity of biologic tissue than standard DWI.

* *Corresponding author*: Giuseppe Cutaia, *cutaiagiuseppe7@gmail.com*
DOI: 10.3269/1970-5492.2020.15.46
 ISSN: 2279-7165 - Available on-line at www.embj.org

Non-Gaussian diffusion of water molecules in biological tissues is quantifiable through the calculation of the apparent kurtosis coefficient (Kapp). Recent investigations have compared DWI and DKI for assessing prostate cancer aggressiveness with inconstant results [7, 9-13].

Therefore, the aim of this study is to compare standard DWI and DKI for distinguishing low-grade (Gleason score =6) from high-grade (Gleason score ≥7) prostate cancers and to explore the diagnostic performance of ADC, ADC-ratio, Kapp and Kapp-ratio for the characterization of prostate lesions on MRI examination using a 1.5T MRI scanner.

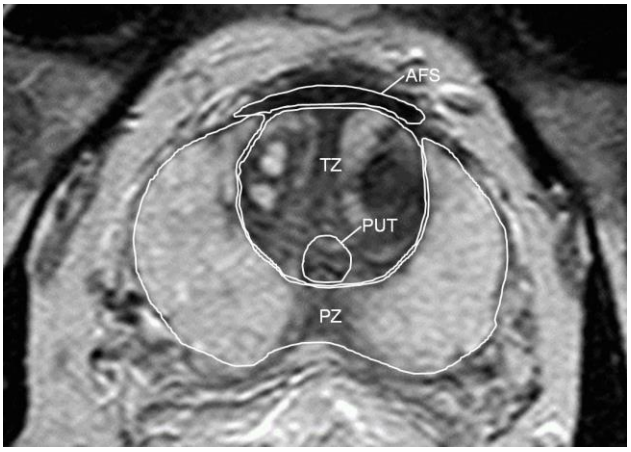

Figure 1. Zonal prostate anatomy on axial T2-weighted MRI image: peripheral zone (PZ) and transitional zone (TZ) are well depicted. Anterior fibromuscular stroma (FMS) and peri-urethral tissue (PUT) are also well detected.

2. Material and methods

This retrospective study was approved by the Institutional Review Board (IRB) of our hospital and written informed consent was waived.

2.1 Population

In the inclusion time between June and December 2018, 75 consecutive patients underwent MRI prostate examination. The MRI scans were performed for one of the following clinical scenarios: (a) increase in serum PSA values (PSA> 4 ng/ml), (b) abnormal findings on digital rectal examination (DRE) or trans-rectal ultrasound (TRUS), (c) systematic biopsy findings of intraepithelial neoplasia (PIN), atypical small acinar proliferation (ASAP) or prostate cancer. Among them, 34 patients were excluded due to prior treatment of prostate cancer or lack of any visible prostate lesion on MRI.

Forty-one patients with PI-RADS score ≥ 3 lesions according to the latest PI-RADS v2.1 algorithm [14] were identified. Seven of these 41 patients were finally excluded due to lack of (n=1) or inadequate (n=6) histopathological results (i.e. non fusion biopsy).

2.2 MRI Technique

The MRI examinations were performed with a 1.5T MRI scanner (Achieva, Philips Healthcare, Best, The Netherlands), using a surface phased array coil (16 channel HD Torso XL). The MRI scans were performed after an interval of at least 6 weeks, if patients had prior prostate biopsy, in order to allow the reabsorption of post-biopsy bleeding foci, a possible source of diagnostic errors. Before each examination, 20 mg of butylscopolamine (Buscopan®, Boehringer-Ingelheim, Ingelheim, Germany) were administered intravenously to suppress intestinal peristalsis. No enema was administered before the examinations.

The morphological study of the gland was performed using Turbo Spin Echo (TSE) T2-weighted sequences acquired on the axial, sagittal and coronal planes, oriented according to the major axis of the prostate. TSE T1-weighted axial sequences were acquired in order to exclude the presence of post-biopsy blood residues, which can be appreciated as hyperintense foci. The DWI and DKI sequences were performed through the acquisition of single-shot ecoplanar sequences (EPI). DWI were acquired at *b* values of 0, 700, 1400 sec/mm^2.

For the DKI sequence, (a single-shot echo-planar imaging with the following parameters: field of view: 350 x 262 mm, matrix: 192 x 130, thickness: 2.7 mm, slice gap: 0.4 mm, number of slices: 20, parallel imaging factor equal to 2) the spread in three directions was calculated with six *b* values (0, 500, 700, 1000, 1400 and 2000 sec/mm^2) in order to obtain a compromise between clinical use and an adequate signal-to-noise ratio (higher *b* values in 1.5T scans degrade image quality). The average acquisition time for DWI and DKI was 3:03 min and 7:43 min, respectively. Sequences obtained were processed using the software integrated in the MRI acquisition workstation in order to obtain the ADC and Kapp maps. The perfusion study was performed after intravenous injection of paramagnetic contrast agent in order to evaluate the presence of hypervascular lesions by acquiring 3D T1-weighted axial sequences after administration of 1 mmol/kg of Gadoteric acid (Dotarem®, Guerbet, USA) at a flow of 3 ml/sec, followed by infusion of 20-30 ml of saline solution. The average acquisition time for standard prostate MRI protocol (not including DKI) was 22:39 min, while prostate MRI with DKI was 30:22 min.

2.3 Imaging analysis

The acquired images and the reports were examined in consensus by two radiologists with 10 and 7 years of experience in prostate imaging, respectively. Images obtained were processed by using dedicated software (MR WorkSpace, Philips Medical System Nederland B.V., The Nederland). Radiologists reviewed the axial T2-weighted and DW images to identify the prostate lesion and traced a region of interest (ROI) encompassing the entire target lesion. Identical ROIs corresponding with the lesion ROI were propagated to both the ADC and Kapp maps (Figure 2). Furthermore, in each patient, a second ROI with the same size was placed in the bladder lumen in order to normalize the values of diffusion and kurtosis coefficients obtained in lesions in relation to that of the bladder urine. The mean value of the ADC and Kapp and the mean value of ADC-ratio and Kapp-ratio calculations for all ROIs were used for the statistical analysis.

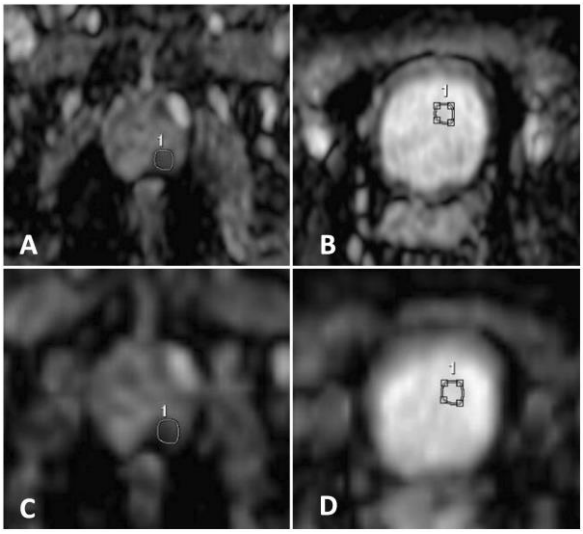

Figure 2. 67-year-old man with PI-RADS 4 lesion in the left peripheral zone. ADC (A, B) and Kapp (C, D) maps show regions of interest traced at the level of the prostate lesion and in the bladder lumen. ADC and Kapp were 0.729 and 0.446, respectively. Targeted fusion biopsy diagnosed Gleason 6 (3 + 3) prostate cancer.

2.4 Histopathological analysis

All patients underwent prostate-targeted fusion biopsy in a period between 2 and 6 weeks after MRI examination using the same technique by a single urologist. Targeted MR-ultrasound fusion biopsy (Esaote MyLab Twice system®, Esaote, Genova, Italy) was performed by taking two biopsy cores from the target lesion, followed, in the same session, by a 12-core transperineal biopsy (sextant and laterally directed biopsies at base, midgland, and apex).

Each specimen obtained from targeted fusion biopsy was considered for this study and histologically analyzed by an experienced pathologist (with >15 years of experience) following the recommendations of the "consensus conference ISUP 2014" [15].

2.5 Statistical analysis

Continuous variables are expressed as mean and standard deviation (SD), and categorical variables are expressed as numbers and percentages.

The Mann-Whitney U test was used to compare the distribution of ADC and Kapp measurements between patients with no prostate cancer and Gleason score equal or higher than 6 (GS≥6) and between patients with Gleason score of 6 (GS=6) and Gleason score equal or higher than 7 (GS≥7). Receiver operating characteristics (ROC) areas under the ROC curve (AUROC) with 95% confidence intervals (CI) and optimal cut-off values based on the Youden index with sensitivity and specificity were calculated to assess the diagnostic performance of ADC and Kapp for the diagnosis of prostate cancer with GS≥6 and GS≥7, respectively.

The correlation between ADC and Kapp measurements, Gleason score of histopathological analysis, and PI-RADS classification at MRI was evaluated using the Spearman's rank correlation coefficient (Spearman's rho). Statistical significance level was set at $p<0.05$. Statistical analysis was conducted using SPSS software (Version 20.0. Armonk, NY, USA: IBM Corp).

3. Results

3.1 Population

Characteristics of the final population are reported in Table 1. The final population consisted of 34 patients, with a mean age of 69 ± 8.1 years (range 49-88 years), each with a prostate lesion confirmed by targeted fusion biopsy. The included lesions were located in the peripheral zone in 28 (82%) cases, while in the transitional zone in the remaining 6 (18%) cases. Overall, there were 6 (18%) PI-RADS 3, 18 (53%) PI-RADS 4 and 10 (29%) PI-RADS 5.

Final histopathological diagnosis revealed no prostate cancer in 11 (32%) patients (1 ASAP+PIN-HG, 1 adenosis, 1 benign prostatic hyperplasia, 8 normal prostatic tissue). Prostate cancer was found in 23 (68%) patients including Gleason score 6 prostate cancer in 8 (24%) lesions, Gleason score 7 prostate cancer in 11 (32%) lesions, Gleason score 8 prostate cancer in 3 (9%) lesions, and Gleason score 9 prostate cancer in 1 (3%) lesion.

Characteristics	
Age (years), mean ± SD (range)	69 ± 8.1 (49-88)
Diameter of lesion (mm), mean ± SD (range)	14.2 ± 6.3 (7-30)
Lesions Location, n (%)	
Transitional zone	6 (18%)
Peripheral zone	28 (82%)
PI-RADS classification, n (%)	
PI-RADS 3	6 (18%)
PI-RADS 4	18 (53%)
PI-RADS 5	10 (29%)
Histopathological diagnosis, n (%)	
No prostate cancer	11 (32%)
Gleason score 6	8 (24%)
Gleason score 7	11 (32%)
Gleason score 8	3 (9%)
Gleason score 9	1 (3%)

Table 1. Characteristics of the included patients.

3.2 Kapp and ADC measurements

Lesions with Gleason score ≥6 had significantly lower Kapp values compared to the lesions disproven to be prostate cancer (0.832 ± 0.184 vs 0.979 ± 0.149, p=0.025) (Table 2, Figure 3a). Contrarily, there was no significant difference between GS≥6 and non-prostate cancer lesions in ADC (0.825 ± 0.112 vs 0.913 ± 0.146, p=0.087), ADC-ratio (0.373 ± 0.066 vs 0.422 ± 0.080, p=0.063) and Kapp-ratio (0.349 ± 0.080 vs 0.405 ± 0.067, p=0.058). When comparing prostate cancers with GS≥7 with lesions having GS=6 (Table 3), the ADC-ratio was the only significantly different parameter (0.362 ± 0.075 vs 0.410 ± 0.067, p=0.039) (Figure 3b), while there was no significant difference in ADC (0.810 ± 0.118 vs 0.888 ± 0.129, p=0.103), Kapp (0.827 ± 0.162 vs 0.920 ± 0.195, p=0.071) or Kapp-ratio (0.341 ± 0.071 vs 0.388 ± 0.081, p=0.064).

Parameters	No prostate cancer	Gleason score ≥6	p-values
ADC	0.913 ± 0.146	0.825 ± 0.112	0.087
Kapp	0.979 ± 0.149	0.832 ± 0.184	**0.025**
ADC-ratio	0.422 ± 0.080	0.373 ± 0.066	0.063
Kapp-ratio	0.405 ± 0.067	0.349 ± 0.080	0.058

Table 2. Differences in apparent diffusion coefficient (ADC) and apparent kurtosis coefficient (Kapp) measurements between Gleason score ≥6 lesions and no prostate cancer lesions. (Variables are expressed as mean and standard deviation and they were compared using the Mann-Whitney U Test. Statistically significant values (p<0.05) are highlighted in bold.)

Parameters	Gleason score =6	Gleason score ≥7	p-values
ADC	0.888 ± 0.129	0.810 ± 0.118	0.103
Kapp	0.920 ± 0.195	0.827 ± 0.162	0.071
ADC-ratio	0.410 ± 0.067	0.362 ± 0.075	**0.039**
Kapp-ratio	0.388 ± 0.081	0.341 ± 0.071	0.064

Table 3. Differences in apparent diffusion coefficient (ADC) and apparent kurtosis coefficient (Kapp) measurements between Gleason score =6 and Gleason score ≥7 prostate cancers. (Variables are expressed as mean and standard deviation and they were compared using the Mann-Whitney U Test. Statistically significant values (p<0.05) are highlighted in bold.)

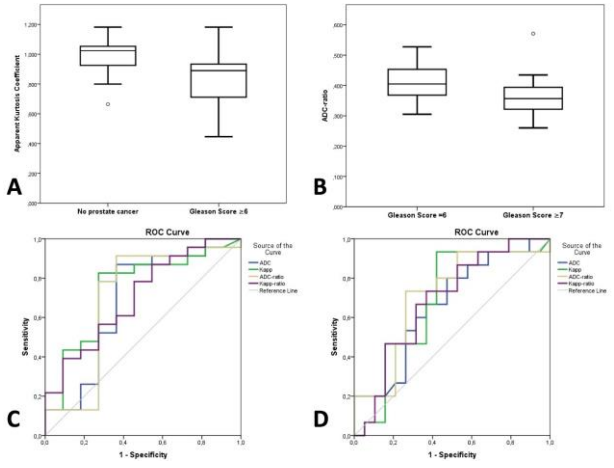

Figure 3. Plot box illustrating the distribution of apparent kurtosis coefficient (Kapp) in lesions with Gleason score ≥6 and no prostate cancer lesions (A); Plot box illustrating the distribution of ADC-ratio in Gleason score =6 and Gleason score ≥7 prostate cancers (B); ROC curve for apparent diffusion coefficient (ADC) and apparent kurtosis coefficient (Kapp) for the diagnosis of GS≥6 lesions (C); ROC curve for apparent diffusion coefficient (ADC) and apparent kurtosis coefficient (Kapp) for the diagnosis of GS≥7 lesions (D).

The performance of ADC and Kapp measurements for the diagnosis of GS≥6 and GS≥7 prostate cancers are reported in Table 4. Corresponding ROC analyses are illustrated in Figure 3c and Figure 3d. Kapp showed the largest area under the receiver operating characteristic curve (AUROC: 0.741, 95% CI: 0.555-0.928, p=0.025) for the diagnosis of GS≥6 lesions.

A Kapp value <0.923 had a sensitivity and specificity of 82.6% and 72.7% for the diagnosis of GS≥6 lesions, respectively. The largest area under the ROC curve for the diagnosis of GS≥7 prostate cancers was achieved by the ADC-ratio (AUROC: 0.709, 95% CI: 0.527-0.891, p=0.039). An ADC-ratio value <0.385 had a sensitivity and specificity of 73.3% and 73.7% for the diagnosis of GS≥7 prostate cancers, respectively.

There was a significant positive correlation (Table 5) between the Kapp and Kapp-ratio measurements with the ADC (Kapp rho=0.666, p<0.001; Kapp-ratio rho=0.662, p<0.001) and ADC-ratio values (Kapp rho=0.656 p<0.001; Kapp-ratio rho=0.722, p<0.001). The correlation between Kapp and ADC is illustrated in Figure 4. Gleason score demonstrated a significant negative correlation with Kapp (rho=-0.392, p=0.022), ADC-ratio (rho=-0.400, p=0.019) and Kapp-ratio (rho=-0.369, p=0.032).

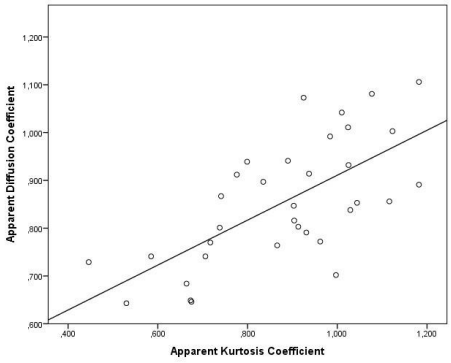

Figure 4. Graphic showing correlation between apparent diffusion coefficient (ADC), apparent kurtosis coefficient (Kapp) measurements (rho=0.666, p<0.001).

Parameters	AUROC	95% CI	P-values	Cut-off	Se (%)	Sp (%)
Gleason score ≥6						
ADC	0.684	0.466-0.901	0.087	<0.923	87.0	63.6
Kapp	0.741	0.555-0.928	0.025	<0.923	82.6	72.7
ADC-ratio	0.700	0.474-0.925	0.063	<0.404	78.3	72.7
Kapp-ratio	0.704	0.515-0.892	0.058	<0.411	78.3	54.5
Gleason score ≥7						
ADC	0.655	0.480-0.850	0.103	<0.894	80.0	52.6
Kapp	0.682	0.494-0.871	0.071	<0.973	93.3	57.9
ADC-ratio	0.709	0.527-0.891	0.039	<0.385	73.3	73.7
Kapp-ratio	0.688	0.507-0.868	0.064	<0.388	73.3	63.2

Table 4. Area under the receiver operating characteristic curve (AUROC), 95% confidence interval (95% CI), sensitivity (Se) and specificity (Sp) and cut-off values based on the Youden index of apparent diffusion coefficient (ADC) and apparent kurtosis coefficient (Kapp) for the diagnosis of GS ≥6 and ≥7 prostate cancers, respectively.

	PI-RADS	Gleason Score	ADC	ADC-ratio
ADC	-0.301	-0.328	-	0.895
p-values	0.084	0.058	-	**<0.001**
Kapp	-0.277	-0.392	0.666	0.656
p-values	0.113	**0.022**	**<0.001**	**<0.001**
ADC-ratio	-0.310	-0.400	0.895	-
p-values	0.074	**0.019**	**<0.001**	-
Kapp-ratio	-0.336	-0.369	0.662	0.722
p-values	0.052	**0.032**	**<0.001**	**<0.001**

Table 5. Correlation between apparent diffusion coefficient (ADC), apparent kurtosis coefficient (Kapp) measurements, PI-RADS classification at multiparametric MRI, and Gleason score. (Numbers represent the Spearman's rank correlation coefficient (rho). Statistically significant values (p<0.05) are highlighted in bold)

4. Discussion and conclusions

Several investigations compared the role of standard DWI and DKI on prostate MRI. However, results in prior studies were discordant as some of them showed additional information about prostate cancer tissue using DKI [17, 18], while others failed to show a difference between DWI and DKI in prostate cancer compared to non-cancer lesions [7, 13, 18, 19]. All these prior studies were conducted using 3.0T MRI scanners so, to our knowledge, this is the first study performed with a 1.5T MRI scanner including both Kapp and Kapp-ratio.

In our study population, we found a statistically significant difference in prostate lesions with GS≥6 compared to lesions proven to be benign only by using Kapp values (p=0.025), while no statistically significant differences were found in ADC values (p=0.087).

Salvaggio et al. [20] reported a statistically significant difference in ADC values between prostate cancer and other lesions (HG-PIN, ASAP).

These differing results can be explained considering that in the present study we divided neoplastic and non-neoplastic lesions, while the prior study considered each non-neoplastic type lesion separately. However, they reported that, even if statistically significant difference was found, there was a high degree of overlap among data [20].

In the present study, only ADC-ratio values allowed both to differentiate between low-grade prostate cancer (GS=6) and high-grade prostate cancer (GS≥7) and significantly correlated with Gleason score (rho=-0.400, p=0.019) while ADC, Kapp and Kapp-ratio values failed to differentiate high grade prostate cancers (GS≥7), although the latter two demonstrated a significant negative correlation (Kapp, rho=-0.392, p=0.022; Kapp-ratio, rho=-0.369, p=0.032) with the Gleason score at histopathological analysis.

Woo et al [21] reported a significant correlation between ADC and ADC-ratio with Gleason score (p<0.001). However, in their study ADC mean value could have been influenced by the large amount of high-grade prostate cancers.

Indeed, with increasing GS, prostate cancer becomes more solid due to the increase in cellular density leading to a modification of ADC values [20]. In our study population we had only three (9%) GS=8 and one (3%) GS=9 prostate cancers which may explain the less significant difference of mean ADC values between low-grade and high-grade prostate cancers.

Our results are consistent with Barrett et al. [19] who reported poor ability of DKI in distinguishing low-grade from high-grade prostate cancers for both peripheral zone (p=0.414-0.825) and transitional zone (p=0.148-0.825). In our study, the high significant correlation between Kapp and ADC (rho=0.666, p<0.001) or ADC-ratio (rho=0.656 p<0.001) with concomitant lack of significant difference of Kapp in high-grade prostate cancer (p=0.071) minimizes its added value compared to the acquisition of standard ADC maps.

Kapp and ADC-ratio showed a fair diagnostic performance for the diagnosis of GS≥6 prostate cancers from no prostate cancer lesions (AUROC of 0.741, p=0.025), and GS≥7 from GS=6 prostate cancers (AUROC of 0.709, p=0.039), respectively. Prior studies have shown discordant results. Wang et al. [11] and Di Trani et al. [16] found that Kapp showed the strongest correlation with Gleason score and the best diagnostic ability in differentiating low-grade from high-grade prostate cancer, according to the ROC analysis. Several studies comparing ADC and ADC-ratio found that ADC-ratio was superior to ADC in determining high-grade prostate cancer [2, 4, 5]. Conversely, other data [3, 21] suggest no additional benefit is gained from using ADC-ratio compared with ADC. Understanding the cause of these different results is challenging. We can hypothesize that different acquisition parameter (highest *b* values ranging from 800 to 1600 mm^2/s), different reference area used for ADC-ratio (peripheral zone, transition zone, tumor zone, urine, or muscle) and clinical and pathologic data (mean age, clinical stage, Gleason score) may be significant contributing factors.

Our study has several limitations that need to be reported. First, our population was small. However, the number of patients in our study (n=34) is in line with prior investigations assessing the value of ADC-ratio, with the exception of the study performed by Woo et al. (n=165) [21]. In our study we do not use endorectal coil for our prostate MRI studies. Endorectal coil is placed directly in close proximity of the posterior circumference of the organ, so a higher signal-to-noise ratio can be achieved.

However, this may lead to increased artifacts [22], anatomical distortion [23], and higher costs. Some studies demonstrated that prostate cancer foci may be detected without decreasing in sensitivity by using a pelvic phase array receiver coil as compared to an endorectal coil [24].

Nevertheless, we needed to select a maximum *b*-value of 2000 sec/mm^2 to maintain the signal-to-noise ratio of the DKI. Higher *b* values are associated with lower signal-to-noise ratios, which may affect the reliability computation of diffusion metrics [14, 25]. However, our study has important clinical implications considering that many installed MRI scanners are built with 1.5T magnet. Another important limitation is that the histological results were obtained after fusion biopsies. Targeted biopsy, as with any biopsy technique, may lead to sampling errors and may misclassify the grade compared to the more robust gold standard of prostatectomy [26].

In conclusion, DKI obtained with 1.5T MRI scanner demonstrated no significant benefit in characterization of prostate cancer lesions on MRI examination compared to standard DWI, although it could be helpful to distinguish prostate cancer from no prostate cancer lesions. ADC, ADC-ratio, Kapp and Kapp-ratio are highly correlated and have similar diagnostic performance.

References

1. Feng Z, Min X, Margolis DJ, Duan C, Chen Y, Sah VK, Chaudhary N, Li B, Ke Z, Zhang P, Wang L. Evaluation of different mathematical models and different b-value ranges of diffusion-weighted imaging in peripheral zone prostate cancer detection using b-value up to 4500 s/mm^2. PLoS One. 2017;12:e0172127.
1. Boesen L, Chabanova E, Logager V, Balslev I, Thomsen HS. Apparent diffusion coefficient ratio correlates significantly with prostate cancer Gleason score at final pathology. J Magn Reson Imaging. 2015;42:446-453.
2. De Cobelli F, Ravelli S, Esposito A, Giganti F, Gallina A, Montorsi F, Del Maschio A. Apparent diffusion coefficient value and ratio as noninvasive potential biomarkers to predict prostate cancer grading: comparison with prostate biopsy and radical prostatectomy specimen. AJR Am J Roentgenol. 2015;204:550-557.
3. Lebovici A, Sfrangeu SA, Feier D, Caraiani C, Lucan C, Suciu M, Elec F, Iacob G, Buruian M. Evaluation of the normal-to-diseased apparent diffusion coefficient ratio as an indicator of prostate cancer aggressiveness. BMC Med Imaging. 2014;14:15.
4. Itatani R, Namimoto T, Yoshimura A, Katahira K, Noda S, Toyonari N, Kitani K, Hamada Y, Kitaoka M, Yamashita Y. Clinical utility of the normalized apparent diffusion coefficient for preoperative evaluation of the aggressiveness of prostate cancer. Jpn J Radiol. 2014;32:685-691.
5. Rosenkrantz AB, Kopec M, Kong X, Melamed J, Dakwar G, Babb JS, Taouli B. Prostate cancer vs. post-biopsy hemorrhage: diagnosis with T2- and diffusion-weighted imaging. J Magn Reson Imaging. 2010;31:1387-1394.
6. Tamada T, Prabhu V, Li J, Babb JS, Taneja SS, Rosenkrantz AB. Prostate Cancer: Diffusion-weighted MR Imaging for Detection and Assessment of Aggressiveness – Comparison between Conventional and Kurtosis Models. Radiology. 2017;284:100-108.
7. Jensen JH, Helpern JA, Ramani A, Lu H, Kaczynski K. Diffusional kurtosis imaging: the quantification of non-gaussian water diffusion by means of magnetic resonance imaging. Magn Reson Med. 2005;53:1432-1440.
8. Rosenkrantz AB, Sigmund EE, Johnson G, Babb JS, Mussi TC, Melamed J, Taneja SS, Lee VS, Jensen JH. Prostate cancer: feasibility and preliminary experience of a diffusional kurtosis model for detection and assessment of aggressiveness of peripheral zone cancer. Radiology. 2012;264:126-135.
9. Suo S, Chen X, Wu L, Zhang X, Yao Q, Fan Y, Wang H, Xu J. Non-Gaussian water diffusion kurtosis imaging of prostate cancer. Magn Reson Imaging. 2014;32:421-427.
10. Wang Q, Li H, Yan X, Wu CJ, Liu XS, Shi HB, Zhang YD. Histogram analysis of diffusion kurtosis magnetic resonance imaging in differentiation of pathologic Gleason grade of prostate cancer. Urol Oncol. 2015;33:337.e15-24.
11. Toivonen J, Merisaari H, Pesola M, Taimen P, Boström PJ, Pahikkala T, Aronen HJ, Jambor I. Mathematical models for diffusion-weighted imaging of prostate cancer using b values up to 2000 s/mm(2) : correlation with Gleason score and repeatability of region of interest analysis. Magn Reson Med. 2005;74:1116-1124.
12. Roethke MC, Kuder TA, Kuru TH, Fenchel M, Hadaschik BA, Laun FB, Schlemmer HP, Stieltjes B. Evaluation of diffusion kurtosis imaging versus standard diffusion imaging for detection and grading of peripheral zone prostate cancer. Invest Radiol. 2015;50:483-489.
13. American College of Radiology website. Prostate imaging reporting & data system (PI-RADS). https://www.acr.org/-/media/ACR/Files/RADS/Pi-RADS/PIRADS-V2-1.pdf?la=en. Accessed 28 July 2020.
14. Epstein JI, Egevad L, Amin MB, Delahunt B, Srigley JR, Humphrey PA, Committee G. The 2014 International Society of Urological Pathology (ISUP) Consensus Conference on Gleason Grading of Prostatic Carcinoma: definition of grading patterns and proposal for a new grading system. Am J Surg Pathol. 2016;40:244-252.
15. Di Trani MG, Nezzo M, Caporale AS, et al. Performance of Diffusion Kurtosis Imaging Versus Diffusion Tensor Imaging in Discriminating Between Benign Tissue, Low and High Gleason Grade Prostate Cancer. Acad Radiol. 2019;26:1328-1337.
16. Li C, Chen M, Wan B, Yu J, Liu M, Zhang W, Wang J. A comparative study of Gaussian and non-Gaussian diffusion models for differential diagnosis of prostate cancer with in-bore transrectal MR-guided biopsy as a pathological reference. Acta Radiol. 2018;59:1395-1402.
17. Wang X, Tu N, Qin T, Xing F, Wang P, Wu G. Diffusion Kurtosis Imaging Combined With DWI at 3-T MRI for Detection and Assessment of Aggressiveness of Prostate Cancer. AJR Am J Roentgenol. 2018;211:797-804.
18. Barrett T, McLean M, Priest AN, Lawrence EM, Patterson AJ, Koo BC, Patterson I, Warren AY, Doble A, Gnanapragasam VJ, Kastner C, Gallagher FA. Diagnostic evaluation of magnetization transfer and diffusion kurtosis imaging for prostate cancer detection in a re-biopsy population. Eur Radiol. 2018;28:3141-3150.
19. Salvaggio G, Calamia M, Purpura P, et al. Role of apparent diffusion coefficient values in prostate diseases characterization on diffusion-weighted magnetic resonance imaging. Minerva Urol Nefrol. 2019;71:154-160.
20. Woo S, Kim SY, Cho JY, Kim SH. Preoperative Evaluation of Prostate Cancer Aggressiveness: Using ADC and ADC Ratio in Determining Gleason Score. AJR Am J Roentgenol. 2016;207:114-120.
21. Barth BK, Cornelius A, Nanz D, Eberli D, Donati OF. Diffusion-Weighted Imaging of the Prostate: Image Quality and Geometric Distortion of Readout-Segmented Versus Selective-Excitation Accelerated Acquisitions. Invest Radiol. 2015;50:785-791.
22. Shah ZK, Elias SN, Abaza R, Zynger DL, DeRenne LA, Knopp MV, Guo B, Schurr R, Heymsfield SB, Jia G. Performance comparison of 1.5-T endorectal coil MRI with 3.0-T nonendorectal coil MRI in patients with prostate cancer. Acad Radiol. 2015;22:467-474.
23. Barth BK, Rupp NJ, Cornelius A, Nanz D, Grobholz R, Schmidtpeter M, Wild PJ, Eberli D, Donati OF. Diagnostic Accuracy of a MR Protocol Acquired with and without Endorectal Coil for Detection of Prostate Cancer: A Multicenter Study. Curr Urol. 2019;12:88-96.
24. Si Y, Liu RB. Diagnostic Performance of Monoexponential DWI Versus Diffusion Kurtosis Imaging in Prostate Cancer: A Systematic Review and Meta-Analysis. AJR Am J Roentgenol. 2018;211:358-368.
25. Lanz C, Cornud F, Beuvon F, Lefèvre A, Legmann P, Zerbib M, Delongchamps NB. Gleason score determination with transrectal ultrasound-magnetic resonance imaging fusion guided prostate biopsies—are we gaining in accuracy? J Urol. 2016;195:88-93.